Research Article | Vol. 26, No. 15 | 23 Jul 2018 | OPTICS EXPRESS 19583
Optics EXPRESS

Quantum metrology beyond Heisenberg limit with entangled matter wave solitons

D. V. Tsarev,[1] S. M. Arakelian,[2] You-Lin Chuang,[3] Ray-Kuang Lee,[3,4] and A. P. Alodjants[1,*]

[1] *National Research University for Information Technology, Mechanics and Optics (ITMO), St. Petersburg 197101, Russia*
[2] *Vladimir State University named after A. G. and N. G. Stoletovs, Gorkii Street 87, Vladimir, Russia*
[3] *Physics Division, National Center for Theoretical Sciences, Hsinchu 30013, Taiwan*
[4] *Institute of Photonics Technologies, National Tsing Hua University, Hsinchu 30013, Taiwan*
[*] *alexander_ap@list.ru*

Abstract: Considering matter wave bright solitons from weakly coupled Bose-Einstein condensates trapped in a double-well potential, we study the formation of macroscopic non-classical states, including Schrödinger-cat superposition state and maximally path entangled $N00N$-state. We examine these macroscopic states by Mach-Zehnder interferometer in the context of parity measurements, which has been done to obtain Heisenberg limit accuracy for linear phase shift measurement. We reveal that the ratio of two-body scattering length to intra-well hopping parameter can be measured with the scaling beyond this limit by using nonlinear phase shift with interacting quantum solitons.

1. Introduction

Nowadays quantum metrology has become one of the fascinating areas in modern quantum physics, which deals with new approaches to the measurement, control, and estimation of physical parameters for achieving ultimate accuracy and exploring all facilities of current quantum technologies [1–9]. Apart from classical measurement theory, a quantum approach predicts the so-called quantum Cramer-Rao (QCR) bound $\langle(\delta\phi_{est})^2\rangle_\phi \geq [\nu F(\phi)]^{-1}$ for estimating arbitrary physical parameter ϕ within a set of ν trials through Fisher information $F(\phi)$ [3,4]. In particular, phase estimation requires high precision measurement, which can be realized both in optical [10–12] and atomic systems [13,14]. The existence of standard quantum limit (SQL) sets a constraint on the linear phase shift (ϕ) measured with the error $\sigma_\phi \sim N^{-1/2}$. Here, N is the average number of particles.

Surpassing SQL in the phase measurement has been demonstrated experimentally with two-mode systems, such as Mach-Zehnder interferometers (MZI), gyroscopes, and lithography devises, where non-classical squeezed or correlated states are applied as the input states [15–19]. For the linear phase measurement, one can achieve the *Heisenberg limit* with the accuracy

$$\sigma_\phi \geq C_0 N^{-1}, \tag{1}$$

which gives the limiting case on QCR bound related to the single mode passing [5,6], C_0 is some constant here. According to the Heisenberg limit approach with non-classical states such as squeezed states, it is required a very large amount of squeezing. Hence, the generation of squeezed states in optical [10–12,20] or atomic [21] physics domain represents one possible solution to improve quantum measurements beyond SQL.

On the other hand, in theory it is proved that for arbitrary two-mode quantum interferometers one can saturate the Heisenberg limit shown in Eq. (1) with maximally entangled N-particle state, coined as $N00N$-state [18,19,22,23]. The $N00N$-states with few photons have been recently observed in quantum optics domain under the spontaneous parametric down conversion

#330272 https://doi.org/10.1364/OE.26.019583
Journal © 2018 Received 25 Apr 2018; revised 30 Jun 2018; accepted 8 Jul 2018; published 19 Jul 2018

Optics EXPRESS

process [24–26]. Alternatively, circuit (or, cavity)-QED devices might be used for these purposes cf. [27–29]. Indeed, atomic $N00N$-states with $N = 2$ atoms have been proposed cf. [29]. Notably, these proposals are based on multi-step quantum state engineering protocols which are sensitive enough to losses and decoherence.

As it is shown in [30–32], in the presence of losses which are modeled by fictitious two beam splitters (BS) with transmissivities $\eta_{1,2}$, the $N00N$-states are not optimal for approaching Heisenberg limit. The optimal (two-component) state, and the $N00N$-state demonstrate approximately equal measurement accuracy, only if $\eta \geq e^{-1/N}$, where $\eta \equiv \eta_1$ is transmissivity of BS in one of the arms; $\eta_2 = 1$. Though in [30, 31] the authors proposed a specific model of losses for photonic interferometers, the fragility problem of $N00N$-states because of the losses become important for a very large particle number N. Thus, the preparation of efficient (robust) mesoscopic $N00N$-states containing a relatively large number of particles and the exploration of them for metrological purposes, are a great challenge and nontrivial task both in theory and experiment [33].

In this work, we propose a method to create $N00N$-states, which are maximally entangled states in path, by means of matter wave bright solitons in Bose-Einstein condensates (BECs). The BEC phenomenon is already demonstrated for the systems in condensed matter and solid state physics, see e.g. [34, 35]. Superfluid properties that occur due to the interaction between condensate particles represent the important feature of the condensates that allows to keep for some time coherence in macroscopically large system regardless of environment even in the presence of weak dissipation [36].

Quantum features of solitons has been extensively studied in optics some times ago [37–44]. In order, squeezing and quantum correlations effects for solitons in optical fibers were demonstrated. However, solitons in such experiments contain huge number of photons (10^8 photons in experiment described by S. Friberg et al [43]) which makes practically impossible to explore them for $N00N$-states formation purposes in the presence of realistic fiber losses.

Remarkably, atomic condensates with negative scattering length might form bright solitons with small number of particles (from several tens to thousands) that allows to treat them quantum mechanically and to consider as suitable candidates for $N00N$-states formation, cf. [45]. The atomic scattering length, that characterizes atom-atom interaction, might be tuned and enhanced by using Feshbach resonance approach [46, 47].

Second, we suggest to use low branch (LB) exciton polariton BECs to produce photonic solitons in quantum domain with the moderate number of photons for quantum metrology purposes. The exciton polaritons are bosonic quasiparticles representing coherent superposition of excitons and photons which occur under the strong coupling condition for a quantum matter-field interaction in high quality semiconductor microstructures. Exciton polariton condensates emit photons at the output of the sample with quantum state that exactly reflects polariton condensate properties. Strong interaction between excitons provides large Kerr-like nonlinearity of polaritonic system that several orders larger than in VCSELs. The number of photons in such solitons might be several tens as is demonstrated in recent experiments with exciton polariton condensate solitons [48]. Notably polariton-polariton interaction might be tuned by Feschbach resonance approach as well [49]. This feature seems to be practically important for quantum measurement applications even in the present of losses, cf. [30, 31].

Relying on the general form of Gross-Pitaevskii equation (GPE) in Heisenberg representation for a condensate in a double-well potential [45], we describe the corresponding quantum field model for coupled bright solitons occurring in two trapped condensates.

Noticing that two condensates admit well-defined relative phase and the total number of particles N which have been examined in a number of experiments and described in the theory, see e.g. [50–55] and cf. [56].

In the framework of quantum field theory [57] we derive the equations of motion for the

Optics EXPRESS

condensate's parameters, i.e., the relative phase and population imbalance between two solitons. Then, we show that the ground state of the system can be a quantum superposition state forming Schrödinger-cat or $N00N$-state. Utilization of these states focused on linear phase shift measurements is revealed for quantum metrology.

Scaling beyond Heisenberg limit, referred as super-Heisenberg scaling, can be achieved in the framework of interaction-based (nonlinear) quantum metrology [7–9, 58–60]. The saturation of the linear Heisenberg limit is demonstrated for nonlinear relative phase parameter estimations for coupled solitons. Our results provide some possible quantum metrology applications beyond linear Heisenberg limit with entangled matter wave solitons.

2. Model for coupled quantum matter bright solitons

Let us consider two BECs, consisting of N particles, trapped in a double-well potential and weakly coupled to each other due to the Josephson effect. This model has been applied for the studies of several effects, i.e. quantum squeezing, entanglement, and related metrology applications for continuous variables within the tight binding approximation [57, 61–65]. Experimentally, such a system can be implemented in atomic optics domain with the help of highly asymmetric potentials, i.e., a cigar-shaped potential [66]. Without the loss of generality, the spatial distribution of the condensates are denoted along z-direction. In addition to the atomic systems, exciton-polariton condensates in the microcavity are also a possible platform for our model [48, 67].

The total Hamiltonian $\hat{H}$ for BECs in a double-well potential can be described by

$$\hat{H} = \hat{H}_1 + \hat{H}_2 + \hat{H}_{int}, \tag{2a}$$

where $\hat{H}_j$ $(j = 1, 2)$ is the Hamiltonian for condensate particles in j-th well; while $\hat{H}_{int}$ accounts for the inter-well coupling between two sites. In the second quantization form we explicitly have

$$\begin{aligned} \hat{H}_j &= \int dz \hat{a}_j(z)^\dagger \left(-\frac{1}{2M}\frac{\partial^2}{\partial z^2} + \frac{U}{2}\hat{a}_j(z)^\dagger \hat{a}_j(z) \right) \hat{a}_j(z) \\ \hat{H}_{int} &= \kappa \int dz \hat{a}_2(z)^\dagger \hat{a}_1(z) + H.C. \end{aligned} \tag{2b}$$

Here, parameter U characterizes two-body interactions, $M = sgn[m_{\text{eff}}] = \pm 1$ is used as the normalized effective particle mass m_{eff}, and κ denotes the inter-well tunneling rate.

In practice bright matter wave solitons with $M = 1, U < 0$ are obtained for atomic condensates with the negative scattering length that corresponds to attractive particles [46, 47]. Contrary, if $M = -1$ and $U > 0$ bright solitons might be formed by the assistance of 1D periodical potential for condensate positive scattering length which is relevant to exciton polariton BECs, or to the atoms with repulsive interaction between the particles [48, 66]. In this case we deal with the negative effective mass of the particles that appear at the edges of Brillouin zone.

The corresponding annihilation (creation) operators of bosonic fields are denoted as $\hat{a}_j$ $(\hat{a}_j^\dagger)$ with $j = 1, 2$, and obey the commutation relations:

$$[\hat{a}_i(z), \hat{a}_j^\dagger(z')] = \delta(z - z')\,\delta_{ij}; \quad i, j = 1, 2. \tag{3}$$

For Hamiltonian (2), we suppose that the ground state of this bosonic system is the product of N single particle states [57]. Physically, this assumption is valid for BECs taken in equilibrium at zero temperature. Thus, the collective ground state for the whole system can be written as:

$$|\Psi\rangle_N = \frac{1}{\sqrt{N!}} \left[\int_{-\infty}^{\infty} dz \left(\Psi_1 \hat{a}_1^\dagger + \Psi_2 \hat{a}_2^\dagger \right) \right]^N |0\rangle, \tag{4}$$

with $|0\rangle \equiv |0\rangle_1 |0\rangle_2$ being a two-mode vacuum state. It is noted that the state vector shown in Eq. (4) relates to the Hartree approach for bosonic systems [37, 38, 68], which is valid for a large

Optics EXPRESS

number of particles N. If we apply the variational approach based on the ansatz $\Psi_1 \equiv \Psi_1(z,t)$ and $\Psi_2 \equiv \Psi_2(z,t)$, with the unknown z-dependent wave-functions, one can have the corresponding Lagrangian density in the form [69]:

$$\begin{aligned} L &= \sum_{j=1}^{2}\left(\frac{i}{2}\left[\Psi_j^*\dot{\Psi}_j - \dot{\Psi}_j^*\Psi_j\right] + \frac{1}{2M}\Psi_j^*\frac{\partial^2\Psi_j}{\partial z^2} - \frac{U}{2}\left|\Psi_j\right|^4\right) \\ &- \kappa\left(\Psi_1^*\Psi_2 + \Psi_1\Psi_2^*\right). \end{aligned} \tag{5}$$

In the limit of vanishing coupling constant $\kappa = 0$, Eq. (5) leads to the well-known GPE, which supports bright soliton solution when $MU < 0$, i.e.,

$$\Psi_j = \frac{N_j}{2}\sqrt{|U|}sech\left(\frac{N_j|U|}{2}z\right)e^{iM\theta_j}. \tag{6}$$

Here N_j is the number of particles in the j-th well and θ_j is the phase, respectively. Below, we take the soliton solutions given in Eq. (6) as our variational ansatz, but imposing time dependent parameters for N_j and θ_j when a weak coupling between the condensates is nonzero. Then, we can obtain the effective Lagrangian by integrating the Lagrangian density (5):

$$\begin{aligned} Ł = &\int_{-\infty}^{\infty} L dz = -M\left(N_1\dot{\theta}_1 + N_2\dot{\theta}_2\right) \\ &+ \frac{U^2}{24M}\left(N_1^3 + N_2^3\right) - \frac{4\kappa N_1 N_2}{N}I(p)\cos\left[\theta\right]. \end{aligned} \tag{7}$$

Here, we have defined $p = (N_2 - N_1)/N$ and $\theta = \theta_2 - \theta_1$ as a population imbalance and phase difference between solitons, respectively. The total number of particles is denoted by $N = N_1 + N_2$. Moreover, we also introduce

$$I(p) = \int_0^{\infty}\frac{dz'}{\cosh^2(z') + \sinh^2(z'p)}. \tag{8a}$$

It is important for analytic analysis that integral defined in Eq.(8) can be approximated by a parabola

$$I(p) \approx 1 - \alpha p^2 \tag{8b}$$

with $\alpha = 0.21$. The direct comparison of (8a) and (8b) with $p \in [0;1]$ has revealed that the maximal relative error of the approximation is about 0.7% for $p = 0.9$.

Basing on Eq. (7) we derived the equation of motions for the population imbalance and phase difference, i.e., p and θ in the form,

$$\dot{p} = -\frac{1}{M}\left(1 - p^2\right)\left(1 - \alpha\, p^2\right)\sin\left[\theta\right], \tag{9a}$$

$$\dot{\theta} = \Lambda p + \frac{2p}{M}\cos\left[\theta\right]\left[1 + \alpha - 2\alpha\, p^2\right]. \tag{9b}$$

Here, the dots denote the derivative with respect to the dimensionless time $t' = 2|\kappa|t$. In Eqs. (9), the dimensionless parameter $\Lambda = \frac{U^2N^2}{16|\kappa|}$ is also introduced, which defines various regimes for BEC behavior in double-well trap.

Two sets of nontrivial stationary solutions can be found for Eqs. (9). For the first set we have

$$p_0^2 = \frac{1}{2\alpha}\left[1 + \alpha - \frac{\Lambda}{2}\right], \tag{10a}$$

$$\cos(\theta_0) = -M; \tag{10b}$$

Optics EXPRESS

and for the second set

$$p_0^2 = 1, \tag{11a}$$

$$\cos\theta_0 = -\frac{M\Lambda}{2(1-\alpha)}. \tag{11b}$$

The first set of nontrivial solutions given in Eqs. (10) is similar to the one obtained under two-mode approximation, and relevant to the tight binding model [57]. However, a vital parameter of system Λ that we have introduced above is proportional to N^2 instead of N which occurs in two-mode limit, cf. [65]. This fact seems to be very important in practice when we consider the limit of the large particle number N, cf. [63]. In the following, we show that this set of solutions can be used to construct Schrödinger-cat state with solitons.

As for the second set of solutions given in Eqs. (11), there is no analogy from the results obtained under two-mode approximation [57, 61–64]. Physically, such a set of solutions implies the formation of $N00N$-state from coupled solitons.

As for the imbalance parameter $0 \leq |p| \leq 1$, the corresponding Λ parameter lies between $2(1-\alpha)$ and $2(1+\alpha)$, resulting in the first set of solutions existing only in $1.58 \leq \Lambda \leq 2.42$. However, for the phase difference $0 \leq |\cos\theta_0| \leq 1$, the second set of solutions can exist for $0 < \Lambda \leq 1.58$ only. One can see that there is a critical value for $\Lambda_{cr} = 2(1-\alpha) \approx 1.58$, at which we have the state with $p^2 = 1$ and $\cos(\theta_0) = -M$. To be more specific, thereafter, we assume $M = 1$.

3. Superposition states of quantum solitons

3.1. Schrödinger-cat state (SC-state)

The SC-state exist at $1.58 \leq \Lambda \leq 2.42$. The state vector of solitons (4) corresponding to Eqs. (10) has the form

$$|\Psi^{(\pm)}\rangle = \frac{1}{\sqrt{N!}}\left[\int_{-\infty}^{\infty} dz \left(\Psi_{\mp}\hat{a}_1^{\dagger} - \Psi_{\pm}\hat{a}_2^{\dagger}\right)\right]^N |0\rangle, \tag{12a}$$

with

$$\Psi_{\pm} = \frac{\sqrt{NU}}{4}(1 \pm |p_0|)sech\left(\frac{NU}{4}(1 \pm |p_0|)z\right), \tag{12b}$$

and $|p_0| = \sqrt{\frac{1}{2\alpha}(1+\alpha-\frac{\Lambda}{2})}$. By defining macroscopic superposition of states from Eqs. (12), we can construct Schrödinger-cat state (SC-state) from coupled solitons, cf. [57]:

$$|\Psi\rangle = C\left(|\Psi^{(+)}\rangle + |\Psi^{(-)}\rangle\right). \tag{13}$$

Here, $C = [2(1+X^N)]^{-1/2}$ is a normalization factor, and $X = \frac{1-p_0^2}{2}\int_{-\infty}^{\infty}\frac{dx}{\cosh[x]+\cosh[p_0 x]} \approx \left(1-p_0^2\right)\left(1-\alpha p_0^2\right)$ with the same $\alpha = 0.21$. Notice that the modes of SC-state (12) are not orthogonal to each other, but follow the relation:

$$\epsilon = \langle\Psi^{(\pm)}|\Psi^{(\mp)}\rangle = X^N. \tag{14}$$

Physically, the *size of the cat* can be defined by $1/\epsilon$ (see Fig. 1(a)). For macroscopic SC-state, we require $\epsilon \ll 1$, which implies the maximally achievable cat size obtained with $|p_0| \to 1$ and $X \to 0$.

Optics EXPRESS

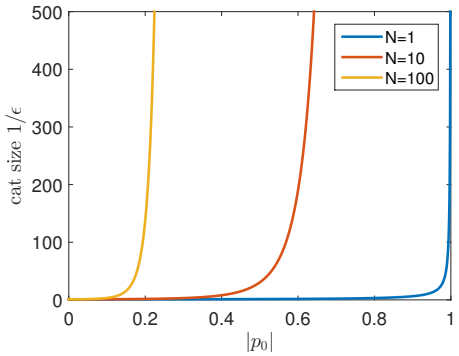

a)

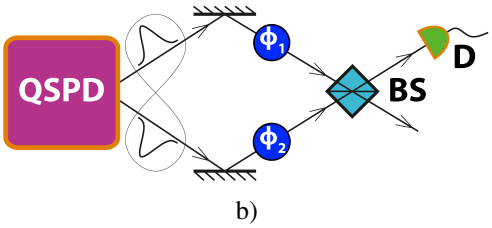

b)

Fig. 1. (a) The dependence of the "cat size" $1/\epsilon$ (14) on the population imbalance $|p_0|$ for different numbers of particles N. One can see that "cat size" tends to infinity when $|p_0|$ tends to 1. Also $1/\epsilon \approx 0$ when $|p_0| \approx 0$. Infinite "cat size" corresponds to macroscopic SC-state and can be approximately taken as a $N00N$-state. Zero "cat size" corresponds to microscopic SC-sate which means almost no entanglement. (b) Illustration of the precision measurement of the phase shift, based on a Mach-Zehnder interferometer (MZI). Here, QSPD denotes a quantum state preparation device, ϕ_1 and ϕ_2 are two resulting phases accumulated at the arms of interferometer, BS is a beam splitter, and D is a parity detector that runs in the particle counting regime.

3.2. $N00N$-state

The $N00N$-state exist at $0 < \Lambda \leq 1.58$. The second set of solutions given in Eqs. (11) presumes the state vector of solitons (4) in the form

$$|\Phi^{(\pm)}\rangle = \frac{1}{\sqrt{N!}}\left[\int_{-\infty}^{\infty} dz \left(\Phi \hat{a}^{\dagger}_{2,1}\right)\right]^N |0\rangle, \tag{15a}$$

with

$$\Phi = \frac{\sqrt{NU}}{2} sech\left(\frac{NU}{2} z\right). \tag{15b}$$

Here we have replaced in notation $|\Psi\rangle \rightarrow |\Phi\rangle$ just for simplicity of the reader's perception. Also the sign $\pm$ here determines modes for $p_0 = \pm 1$. The superposition state constructed from Eqs. (15) is:

$$|\Phi\rangle = \frac{1}{\sqrt{2}}\left(|\Phi^{(+)}\rangle + e^{-i\theta_N}|\Phi^{(-)}\rangle\right), \tag{16}$$

which clearly gives us a $N00N$-state of solitons. Here, we also introduce $\theta_N = N\theta_0 = N \arccos\left(-\frac{\Lambda}{2(1-\alpha)}\right)$.

At the critical value of $\Lambda = \Lambda_{cr} = 1.58$, the SC-state shown in Eq. (13) transformes into the $N00N$-state described by Eq. (16), with $\theta_0 = \pi$ phase difference between two solitons.

4. Quantum measurements with superposition states

In this section we propose a precision measurement experiment with SC-state and $N00N$-state. The Mach-Zehnder interferometer (MZI) is illustrated in Fig. 1(b). The device coined as a quantum state preparation device (QSPD) represents the medium with two coupled BECs producing entangled soliton states (may be the superposition state, SC-state or $N00N$-state) into

Optics EXPRESS

the input of a MZI. The measured parameter is a linear phase shift $\phi = \phi_2 - \phi_1$ accumulated in the arms of MZI.

Experimental realization of the scheme in Fig. 1(b)with atomic condensates is based on the so-called method of nonlinear Ramsey interferometry that is performed in time domain, cf. [14]. First the method implies the formation of two entangled solitons composing $N00N$-state in our case. Then, the total state undergoes free evolution. BS combines modes for the readout by applying $\pi/2$ microwave pulse to atomic cloud which couples two internal atomic states.

As it is demonstrated in [70], the current micro- and nanotechnologies allow to design semiconductor based MZI operating with exciton polariton condensates and possessing optically controlable phase shift, polarization, output intensity that opens the door for quantum optical metrology purposes being under discussion.

The sensitivity of the phase parameter ϕ for the scheme in Fig. 1(b)is determined by (cf. [71])

$$\langle(\Delta\phi)^2\rangle = \frac{\langle\left(\Delta\hat{P}\right)^2\rangle}{\left|\frac{\partial\langle\hat{P}\rangle}{\partial\phi}\right|^2}, \tag{17}$$

where, $\hat{P}$ is a Hermitian operator suitable for the measurement of the phase ϕ. We propose to use a parity detection procedure with the operator taken for the second mode: $\hat{P} \equiv \hat{P}_{\hat{a}_2} = \exp\left[i\pi\int_{-\infty}^{\infty}\hat{a}_2^\dagger\hat{a}_2 dz\right]$. For this purpose, for parity measurement shown in Fig. 1(b), two matter waves are combined at the BS after phase-shifting operations, and then one of the detectors counts the even or odd number of particles.

Though, at present, parity measurement experimentally represents a non-trivial task requiring high efficiency particle-number counting (resolving) detectors, it is absolutely imperative to achieve Heisenberg scaling by phase measurement in our scheme, cf. [73]. Notably, in the recent experiment it was demonstrated that super-resolution phase measurement was 144 times better than the Rayleigh limit for coherent photonic states in MZI, obtaned by measuring photon number parity as a readout [74]. To describe the parity measurement, one may introduce the following spin operators

$$\hat{S}_0 = \frac{1}{2}\int_{-\infty}^{\infty}\left(\hat{a}_1^\dagger\hat{a}_1 + \hat{a}_2^\dagger\hat{a}_2\right)dz, \tag{18a}$$

$$\hat{S}_1 = \frac{1}{2}\int_{-\infty}^{\infty}\left(\hat{a}_1^\dagger\hat{a}_1 - \hat{a}_2^\dagger\hat{a}_2\right)dz, \tag{18b}$$

$$\hat{S}_2 = \frac{1}{2}\int_{-\infty}^{\infty}\left(\hat{a}_1^\dagger\hat{a}_2 + \hat{a}_2^\dagger\hat{a}_1\right)dz, \tag{18c}$$

$$\hat{S}_3 = \frac{i}{2}\int_{-\infty}^{\infty}\left(\hat{a}_2^\dagger\hat{a}_1 - \hat{a}_1^\dagger\hat{a}_2\right)dz. \tag{18d}$$

These operators obey $SU(2)$ algebra and to commutation relations: $[\hat{S}_i, \hat{S}_j] = i\epsilon_{ijk}\hat{S}_k$, with $i, j, k = 1, 2, 3$. Having $\hat{S}_j$ operators we can define unitary operators for the transformations of quantum state in the beam splitter and phase shift, i.e., $\hat{U}_{BS} = \exp\left[i\frac{\pi}{2}\hat{S}_2\right]$ and $\hat{U}_{PS} = \exp\left[-i\phi\hat{S}_1\right]$, respectively. Then, the action of MZI on initial quantum state can be described by MZI-operator, i.e., $\hat{U}_{MZI} = \hat{U}_{BS}\hat{U}_{PS} = \exp\left[i\frac{\pi}{2}\hat{S}_2\right]\exp\left[-i\phi\hat{S}_1\right]$. The parity operator $\hat{P}_{a_2}$ in this formalism has the form:

$$\hat{P}_{\hat{a}_2} \equiv \exp\left[i\pi(\hat{S}_0 - \hat{S}_1)\right]. \tag{19}$$

Thus, for the scheme shown in Fig. 1(b), the resulting expectation value of parity operator $\hat{P}_{a_2}$ can be calculated as

$$\langle\hat{P}_{\hat{a}_2}\rangle = \langle\hat{U}_{MZI}^\dagger\hat{P}_{a_2}\hat{U}_{MZI}\rangle = \langle e^{i\pi\hat{S}_0}e^{i\phi\hat{S}_1}e^{i\pi\hat{S}_3}e^{-i\phi\hat{S}_1}\rangle. \tag{20}$$

Optics EXPRESS

It is also more convenient to use the angular momentum state representation instead of the particle number representation. Here, we consider the following substitution $|N_1, N_2\rangle \rightarrow |j, m\rangle$, where N_1, N_2 are numbers of particles in the first and second wells. The quantum numbers for angular momenta j and m are introduced as $j = N/2$ and $m = (N_1 - N_2)/2$, respectively. The states $|j, m\rangle$ are eigenstates of the spin operators $\hat{S}_{0,1}$ with the conditions $\hat{S}_1|j, m\rangle = m|j, m\rangle$; $\hat{S}_0|j, m\rangle = j|j, m\rangle$and $\exp[i\pi S_3]|N_1, N_2\rangle = \exp[i\pi N_1]|N_2, N_1\rangle$.

In terms of the angular momentum we can rewrite SC-state in Eq. (13) and $N00N$-state Eq. (16) as

$$|\Psi\rangle = C\left(|j, -m\rangle + |j, m\rangle\right), \tag{21a}$$

$$|\Phi\rangle = \frac{1}{\sqrt{2}}\left(|j, -j\rangle + e^{-i\theta_N}|j, j\rangle\right). \tag{21b}$$

Then the resulting average value $\langle\hat{P}_{a_2}\rangle$ for initial SC-state and $N00N$-state, respectively, have the form:

$$\langle\Psi|\hat{P}_{\hat{a}_2}|\Psi\rangle = (-1)^N \cos\left[\left(\phi - \frac{\pi}{2}\right)N|p_0|\right], \tag{22a}$$

$$\langle\Phi|\hat{P}_{\hat{a}_2}|\Phi\rangle = \begin{cases}(-1)^{\frac{N}{2}}\cos\left[\phi N + \theta_N\right]; & N \text{ is even}\\ (-1)^{\frac{N+1}{2}}\sin\left[\phi N + \theta_N\right]; & N \text{ is odd}\end{cases} \tag{22b}$$

with the variation $\langle(\Delta\hat{P}_{\hat{a}_2})^2\rangle$:

$$\langle\Psi|(\Delta\hat{P}_{\hat{a}_2})^2|\Psi\rangle = \sin^2\left[\left(\phi - \frac{\pi}{2}\right)N|p_0|\right], \tag{23a}$$

$$\langle\Phi|(\Delta\hat{P}_{\hat{a}_2})^2|\Phi\rangle = \begin{cases}\sin^2\left[\phi N + \theta_N\right]; & N \text{ is even}\\ \cos^2\left[\phi N + \theta_N\right]; & N \text{ is odd}\end{cases} \tag{23b}$$

From the results above, we can see that quantum interference effects arise in the parity measurement scheme depending on the even or odd particle numbers N. As for the sensitivity of interferometer, we immediately obtain from Eq. (17)

$$\langle\Psi|(\Delta\phi)^2|\Psi\rangle = \frac{1}{N^2|p_0|^2}, \tag{24a}$$

$$\langle\Phi|(\Delta\phi)^2|\Phi\rangle = \frac{1}{N^2}. \tag{24b}$$

One can see that the Heisenberg limit is achieved for a maximally entangled $N00N$-state and the precision for SC-state has an extra $1/|p_0|^2$ factor. In Fig. 2(a), we plot a normalized error in the phase measurement $\sigma_\phi = \sqrt{\langle(\Delta\phi)^2\rangle}$ as a function of particle number N for SC-state. The value $\sigma_\phi = N^{-1/2}$ characterizes SQL of the phase measurement with classical states, which can be achieved without QSPD. One can see that the accuracy of measurement tends to the Heisenberg limit as the cat size grows and is saturated by $|p_0| = 1$ at the input (the yellow curve in Fig. 2(a)). On the contrary, a microscopic SC-state obtained when $|p_0| \rightarrow 0$ is not suitable to perform the measurements.

5. Measurements beyond the Heisenberg scaling

The accuracy of measurement can be improved even more by using parameters with nonlinear particle number dependence. In the framework of nonlinear interferometry, the arbitrary Θ-parameter measurement procedure uses transformation $|\Psi\rangle_\Theta = \exp(i\Theta G)|\Psi\rangle$ for input state

Optics EXPRESS

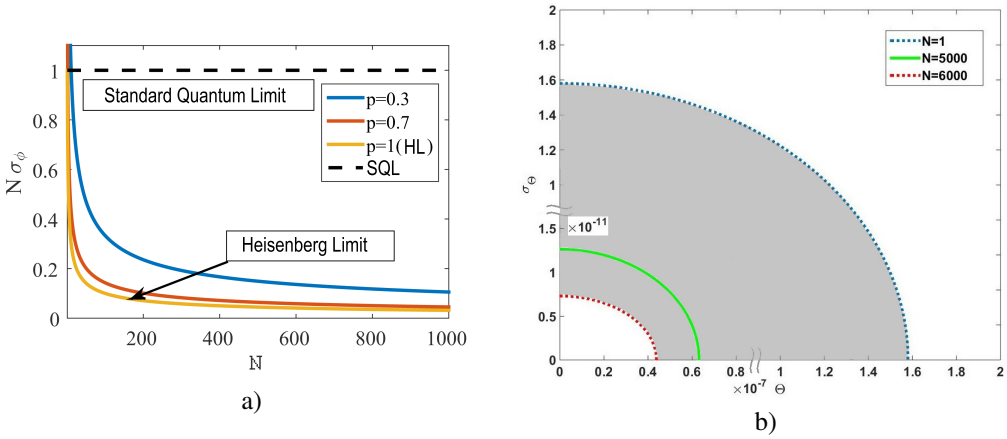

Fig. 2. (a) Reduced phase uncertainty $\sqrt{N}\sigma_\phi$ against total particle number N, for an initial SC-state used in the measurement procedure. The value $\sqrt{N}\sigma_\phi = 1$ corresponds to SQL limit. (b) The dependence of σ_Θ on Θ demonstrating a second-order like phase transition from the state possessing non-zero σ_Θ beyond the linear Heisenberg limit (gray area) to the state nonapplicable for such measurements. The number of particles $N = N_c = 6000$ is taken for Lithium atomic condensates with negative scattering length, as example.

$|\Psi\rangle$, where G is the generator of transformation that describe nonlinear phase dependence, cf. [7–9, 58, 60].

In the general case for $G = N^k$ the ultimate sensitivity of the Θ-parameter measurement in a nonlinear interferometer is bound by the value $\sigma_\Theta \simeq 1/N^k$, which corresponds to the so-called super-Heisenberg limit for the phase measurement in quantum metrology, cf. [59].

To be more specific, we focus on so-called interaction-based quantum metrology approach where we use light-matter (nonlinear) quantum interface for quantum noise-limited interactions, cf. [59]. The Θ-parameter that characterizes relative strength U of nonlinear inter-particle interaction in each well with respect to the linear inter-well coupling coefficient κ is the subject of high precision measurement beyond Heisenberg limit: $\Theta = \frac{\Lambda}{N^2} = \frac{U^2}{16|\kappa|}$. Noticing that Θ does not depend on number of particle N which means resistance of such experiment to particle losses. The Θ- parameter measurement can be performed in the same way as for phase-shift ϕ measurement in Fig. 1(b) by accounting only soliton phase difference

$$\theta_N = N \arccos\left(-\frac{\Theta N^2}{2(1-\alpha)}\right), \tag{25}$$

for prepared initially $N00N$-state, see Eqs. (16, 17).

For a sufficiently small Θ, which implies large value of N, we can apply the Taylor expansion

$$\theta_N = \frac{\pi}{2}N + \frac{N^3}{2(1-\alpha)}\Theta + O(\Theta^3), \tag{26}$$

which is valid as long as we take into account only a linear dependence on Θ. Setting $\phi = 0$ for

Optics EXPRESS

neglecting unimportant phase shift, we have for the $N00N$-state at the input of the MZI:

$$\langle\Phi|\hat{P}_{\hat{a}_2}|\Phi\rangle = \begin{cases} (-1)^{\frac{N}{2}}\cos\left[\theta_N\right]; & N \text{ is even} \\ (-1)^{\frac{N+1}{2}}\sin\left[\theta_N\right]; & N \text{ is odd} \end{cases} \tag{27a}$$

$$\langle\Phi|(\Delta\hat{P}_{\hat{a}_2})^2|\Phi\rangle = \begin{cases} \sin^2\left[\theta_N\right]; & N \text{ is even} \\ \cos^2\left[\theta_N\right]; & N \text{ is odd} \end{cases} \tag{27b}$$

for the average value of $\hat{P}_{a_2}$ and the corresponding variance, respectively. The resulting sensitivity of Θ can be found to be:

$$\langle(\Delta\Theta)^2\rangle = \frac{4(1-\alpha)^2}{N^6}. \tag{28}$$

From Eq. (28), the error in Θ is $\sigma_\Theta = \sqrt{\langle(\Delta\Theta)^2\rangle} \sim N^{-3}$ that looks quite promising for improving measurement sensitivity which currently achieved with atomic condensates, cf. [59, 65, 66].

In Fig. 2(a)), we show the dependence of σ_Θ as a function of measured Θ-parameter, for different particle numbers N. The blue dashed-curve in Fig. 2(a)corresponds to the ultimate measurements with one particle. The shadowed region in Fig. 2(a))reveals the capacity for the measurements with particle number $1 \leq N \leq 6000$. The maximal number of particles in the condensate is limited by the number N_c that corresponds to particle number in collapsing condensate possessing negative scattering length, cf. [45]. Obviously, for $N > N_c$ the system become dynamically unstable especially for macroscopic quantum states superposition discussed in the paper.

6. Conclusion

In summary, accepting a quantum field theory approach to the problem of bright matter wave soliton formation in weakly coupled double-well potentials, we reveal the ground states in the Schrödinger-cat superposition state (SC-state) and maximally path entangled $N00N$-state. With the variational method, we derive the equation of motions for SC-state and $N00N$-state. Then, within the Mach-Zehnder interferometer we examine quantum phase measurement with these superposition states, in order to have the accuracy beyond the standard quantum limit and the linear Heisenberg limit. We perform the $\hat{P}_{\hat{a}_2}$ operator measurements by applying a parity measurement procedure. Heisenberg-limited phase shift measurements are demonstrated to be saturated for maximally path entangled state containing N particles. A vital combination of condensate parameters $\Theta = \frac{U^2}{16|\kappa|}$ is shown to surpass the linear Heisenberg limit in terms of the nonlinear metrology approach, when scaling is proportional to N^{-3}. These results applied to atomic $N00N$-states represent a promising tool for atomic clocks and atomic gyroscopes [65, 66].

Notably, decoherence effects play an important role for the schemes operating with SC-states and/or $N00N$-states, cf. [72]. From the practical point of view it is more important to identify characteristic time scales when superposition states and – more generally – two component macroscopic condensates might be implemented for quantum operations. Contrary to standard (single particle) qubits, as it is shown in [75], the required time of gate operation in condensates for producing entanglement is inversely proportional to the particle number N. This enhancement is achieved due to bosonic stimulation effect and implies a fast quantum gate operation. Obviously, decoherence effects occurring in condensate macroscopic states should appear at longer time.

Remarkably, condensate quantum solitons pose some specific peculiarities during their propagation in the presence of decoherence, via one-, two-, and/or three-body losses cf. [76]. In the paper we are examining bright solitons at rest. Obviously, the analysis of motional degree of freedom seems to be important due to the uncertainty relation for soliton momentum and position [37, 38]. One of the possible realizations of the scheme represented in Fig. 2 is connected

Optics EXPRESS

with exciton-polariton bright solitons propagation in high-Q semiconductor microcavities [48, 70]. The lifetime of solitons is several tens of picoseconds that is large enough as compared to the possible quantum operation. Moreover, recently there were proposed by Y. Sun *et al.* in [77] few hundred picoseconds lifetime for LB exciton polaritons in semiconductor microstructures. This enables to avoid decoherence and undesirable spreading effects for characteristic long lifetimes [37, 38, 76]. In other words, long-lived exciton polariton condensates can be a new platform for designing maximally entangled states with moving solitons. These problems will be a subject of intensive study both in theory and experiment in forthcoming papers.

Funding

Government of Russian Federation, Grant No. 08-08 and the Ministry of Science and Technology of Taiwan under Grant No. 105-2628-M-007-003-MY4.

References

1. H. M. Wiseman and G. J. Milburn, *Quantum Measurement and Control* (Cambridge University, 2010).
2. C. E. Wieman, D. E. Pritchard, and D.J. Wineland, "Atom cooling, trapping, and quantum manipulation," Rev. Mod. Phys. **71**, S253 (1999).
3. R. Demkowicz-Dobrzanski, M. Jarzyna, J. Kolodynski, "Quantum limits in optical interferometry," Progress in Optics **60**, 345–435 (2015).
4. J. P. Dowling and K. P. Seshadreesan, "Quantum Optical Technologies for Metrology, Sensing, and Imaging," J. of Lightwave Tech. **33**, 2359–2370 (2015).
5. V. Giovannetti, S. Lloyd, and L. Maccone, "Quantum-Enhanced Measurements: Beating the Standard Quantum Limit," Science **306**, 1330–1336 (2004).
6. V. Giovannetti, S. Lloyd, and L. Maccone, "Advances in quantum metrology," Nature Photon. **5**, 222–229 (2011).
7. S. M. Roy and S. L. Braunstein, "Exponentially Enhanced Quantum Metrology," Phys. Rev. Lett. **100**, 220501 (2008).
8. S. Boixo, Steven T. Flammia, C. M. Caves, and J.M Geremia, "Generalized Limits for Single-Parameter Quantum Estimation," Phys. Rev. Lett. **98**, 090401 (2007).
9. S. Boixo, A. Datta, M. J. Davis, S. T. Flammia, A. Shaji, and C. M. Caves, "Quantum Metrology: Dynamics versus Entanglement," Phys. Rev. Lett. **101**, 040403 (2008).
10. C. M. Caves, "Quantum-mechanical noise in an interferometer," Phys. Rev. D **23**, 1693 (1981).
11. B. Yurke, S. L. McCall, and J. R. Klauder, "SU(2) and SU(1,1) interferometers," Phys. Rev. A **33**, 4033 (1986).
12. P. Grangier, R. E. Slusher, B. Yurke, and A. LaPorta, "Squeezed-light-enhanced polarization interferometer," Phys. Rev. Lett. **59**, 2153 (1987).
13. T. L. Gustavson, P. Bouyer, and M. A. Kasevich, "Precision Rotation Measurements with an Atom Interferometer Gyroscope," Phys. Rev. Lett. **78**, 2046 (1997).
14. C. Gross, T. Zibold, E. Nickolas, J. Estève, M.K. Oberthaler, "Nonlinear atom interferometer surpasses classical precision limit," Nature **464**, 1165–1169 (2010).
15. J. P. Dowling, "Correlated input-port, matter-wave interferometer: Quantum-noise limits to the atom-laser gyroscope," Phys. Rev. A **57**, 4736 (1998).
16. D. J. Wineland, J. J. Bollinger, W. M. Itano, F. L. Moore, and D. J. Heinzen, "Spin squeezing and reduced quantum noise in spectroscopy," Phys. Rev. A **46**, R6797 (1992).
17. J. J. Bollinger, W. M. Itano, D. J. Wineland, and D. J. Heinzen, "Optimal frequency measurements with maximally correlated states," Phys. Rev. A **54**, R4649 (1996).
18. A. N. Boto, P. Kok, D. S. Abrams, S. L. Braunstein, C. P. Williams, and J. P. Dowling,"Quantum Interferometric Optical Lithography: Exploiting Entanglement to Beat the Diffraction Limit," Phys. Rev. Lett. **85**, 2733 (2000).
19. P. Kok, S.L. Braunstein, and J. P. Dowling, "Quantum lithography, entanglement and Heisenberg-limited parameter estimation," J. Opt. B: Quantum Semiclass. Opt. **6**, S811 (2004).
20. H. Vahlbruch, M. Mehmet, K. Danzmann, and R. Schnabel, "Detection of 15 dB Squeezed States of Light and their Application for the Absolute Calibration of Photoelectric Quantum Efficiency," Phys. Rev. Lett. **117**, 110801 (2016).
21. J. Esteve, C. Gross, A. Weller, S. Giovanazzi and M. K. Oberthaler, "Squeezing and entanglement in a BoseâĂŞEinstein condensate," Nature **455**, 1216 (2008).
22. J. P. Dowling, "Quantum optical metrology - the lowdown on high-N00N states," Contem. Phys. **49**, 125–143 (2008).
23. L. Pezze and A. Smerzi, "Mach-Zehnder Interferometry at the Heisenberg Limit with Coherent and Squeezed-Vacuum Light," Phys. Rev. Lett. **100**, 073601 (2008).
24. Heonoh Kim, Hee Su Park, and Sang-Kyung Choi, "Three-photon N00N states generated by photon subtraction from double photon pairs," Optics Express **17**, 19720–19726 (2009).
25. I. Afek, O. Ambar, and Y. Silberberg, "High-NOON States by Mixing Quantum and Classical Light," Science **328**, 879–881 (2010).

Optics EXPRESS

26. L. A. Rozema, J. D. Bateman, D. H. Mahler, R. Okamoto, A. Feizpour, A. Hayat, and A. M. Steinberg, "Scalable Spatial Superresolution Using Entangled Photons," Phys. Rev. Lett. **112**, 223602 (2014).
27. S. T Merkel, and F. K Wilhelm, "Generation and detection of NOON states in superconducting circuits," New Journal of Physics **12**, 093036 (2010).
28. Qi-Ping Su, Chui-Ping Yang and Shi-Biao Zheng, "Fast and simple scheme for generating NOON states of photons in circuit QED," Scientific Reports **4**, 3898 (2014).
29. Yu-Ao Chen, Xiao-Hui Bao, Zhen-Sheng Yuan, Shuai Chen, Bo Zhao, and Jian-Wei Pan, "Heralded Generation of an Atomic NOON State," Phys. Rev. Letts **104**, 043601 (2010).
30. U. Dorner, R. Demkowicz-Dobrzanski, B. J. Smith, J. S. Lundeen,W.Wasilewski, K. Banaszek, and I. A.Walmsley, "Optimal Quantum Phase Estimation," Phys. Rev. Lett. **102**, 102, 040403 (2009).
31. K. Banaszek, R.Demkowicz-Dobrzaski and I. A. Walmsley, "Quantum states made to measure," Nature Photonics **3**, 673 (2009).
32. J. Kolodyski and R. Demkowicz-Dobrzaski, "Efficient tools for quantum metrology with uncorrelated noise," New J. Phys. **15** 073043 (2013).
33. Jaewoo Joo, W.J. Munro, and T. P. Spiller, "Quantum Metrology with Entangled Coherent States," Phys. Rev. Lett. **107**, 083601 (2011).
34. A. J. Leggett, "Bose-Einstein condensation in the alkali gases: Some fundamental concepts," Rev. Mod. Phys. **73**, 307–357 (2001).
35. Hui Deng, H. Haug, and Yoshihisa Yamamoto, "Exciton-polariton Bose-Einstein condensation," Rev. Mod. Phys. **82**, 1489 (2010).
36. I. Carusotto and C. Ciuti, "Quantum fluids of light," Rev. Mod. Phys. **88**, 299 (2013).
37. Y. Lai and H. A. Haus, "Quantum theory of solitons in optical fibers. I. Time-dependent Hartree approximation," Phys. Rev. A **40**, 844 (1989).
38. Y. Lai and H. A. Haus, "Quantum theory of solitons in optical fibers. II. Exact solution," Phys. Rev. A **40**, 854 (1989).
39. P. D. Drummond and S. J. Carter, "Quantum-field theory of squeezing in solitons," J. Opt. Soc. Am. B **4**, 1565 (1987).
40. S. Carter, P. Drummond, M. Reid, and R. Shelby, "Squeezing of quantum solitons," Phys. Rev. Lett. **58**, 1841 (1987).
41. M. Rosenbluh and R. M. Shelby, "Squeezed optical solitons," Phys. Rev. Lett. **6**, 153 (1991).
42. M. Shirasaki, H. A. Haus, "Squeezing of pulses in a nonlinear interferometer," J. Opt. Soc. Am. B **7**, 30 (1990).
43. S. R. Friberg, S. Machida, M. J. Werner, A. Levanon, and Takaaki Mukai, "Observation of Optical Soliton Photon-Number Squeezing," Phys. Rev. Lett. **77**, 3775 (1996).
44. S. Spälter, N. Korolkova, F. König, A. Sizmann, and G. Leuchs, "Observation of Multimode Quantum Correlations in Fiber Optical Solitons," Phys. Rev. Lett. **81**, 786 (1998).
45. C. J. Pethick and H. Smith, *Bose-Einstein Condensation in Dilute Gases,* (Cambridge University, 2008).
46. K. E. Strecker, G. B. Partridge, A. G. Truscott, and R. G. Hulet, "Formation and propagation of matter-wave soliton trains," Nature **417**, 150–153 (2002).
47. L. Khaykovich, F. Schreck, G. Ferrari, T. Bourdel, J. Cubizolles, L. D. Carr, Y. Castin, and C. Salomon, "Formation of a Matter-Wave Bright Soliton," Science **296**, 1290–1293 (2002).
48. M. Sich, D. N. Krizhanovskii, M. S. Skolnick, A. V. Gorbach, R. Hartley, D. V. Skryabin, E. A. Cerda-Méndez, K. Biermann, R. Hey, and P. V. Santos, "Observation of bright polariton solitons in a semiconductor microcavity," Nat. Photon. **6**, 50–55 (2012).
49. N. Takemura, S. Trebaol, M.Wouters, M. T. Portella-Oberli and B. Deveaud, "Polaritonic Feshbach resonance", Nat. Phys. **10**, 500 (2014).
50. M.R. Andrews, C.G. Townsend, H. Miesner, D.S. Durfee, D.M. Kurn, W. Ketterle, "Observation of Interference Between Two Bose Condensates," Science **275**, 637–641 (1997).
51. B. P. Anderson, M. A. Kasevich, "Macroscopic quantum interference from atomic tunnel arrays," Science **282**, 1686–1689 (1998).
52. S. Kohler and F. Sols, "Phase-resolution limit in the macroscopic interference between Bose-Einstein condensates," Phys. Rev. A, **63**, 053605 (2001).
53. J. Javanainen and M. Wilkens, "Phase and Phase Diffusion of a Split Bose-Einstein Condensate," Phys. Rev. Lett. **78**, 4675 (1997).
54. I. Zapata, F. Sols, and A. J. Leggett, "Josephson effect between trapped Bose-Einstein condensates," Phys. Rev. A **57**, R28(R) (1998).
55. Y. Castin and J. Dalibard, "Relative phase of two Bose-Einstein condensates," Phys. Rev. A, **55**, 4330 (1997).
56. A. M. Dudarev, M. G. Raizen, and Qian Niu, "Quantum Many-Body Culling: Production of a Definite Number of Ground-State Atoms in a Bose-Einstein Condensate," Phys. Rev. Lett. **98**, 063001 (2007).
57. J. I. Cirac, M. Lewenstein, K. Mølmer, and P. Zoller, "Quantum superposition states of Bose-Einstein condensates," Phys. Rev. A **57**, 1208 (1998).
58. J. Beltran and A. Luis, "Breaking the Heisenberg limit with inefficient detectors," Phys. Rev. A **72**, 045801 (2005).
59. M. Napolitano, M. Koschorreck, B. Dubost, N. Behbood, R. J. Sewell, and M. W. Mitchell, "Interaction-based quantum metrology showing scaling beyond the Heisenberg limit," Nature **471**, 486–489 (2011).
60. D. Maldonado-Mundo and A. Luis, "Metrological resolution and minimum uncertainty states in linear and nonlinear signal detection schemes," Phys. Rev. A **80**, 063811 (2009).
61. A. Sorensen, L.-M. Duan, J. I. Cirac and P. Zoller, "Many-particle entanglement with Bose-Einstein condensates,"

Optics EXPRESS

Nature **409**, 63–66 (2001).
62. L. Fu and J. Liu, "Quantum entanglement manifestation of transition to nonlinear self-trapping for Bose-Einstein condensates in a symmetric double well," Phys. Rev. A **74**, 063614 (2006).
63. G. Mazzarella, L. Salasnich, A. Parola, and F. Toigo, "Coherence and entanglement in the ground state of a bosonic Josephson junction: From macroscopic Schrödinger cat states to separable Fock states," Phys. Rev. A **83**, 053607 (2011).
64. Q. Y. He, P. D. Drummond, M. K. Olsen, and M. D. Reid, "Einstein-Podolsky-Rosen entanglement and steering in two-well Bose-Einstein-condensate ground states," Phys. Rev. A **86**, 023626 (2012).
65. L. Pezze, A. Smerzi, M. K. Oberthaler, R. Schmied, and P. Treutlein, "Quantum metrology with nonclassical states of atomic ensembles," arXiv:1609.01609 (2016).
66. O. Morsch and M. Oberthaler, "Dynamics of Bose-Einstein condensates in optical lattices," Rev. Mod. Phys. **78**, 179 (2006).
67. C. Schneider, K. Winkler, M. D. Fraser, M. Kamp, Y. Yamamoto, E. A. Ostrovskaya, and S. Hofling, "Exciton-polariton trapping and potential landscape engineering," Rep. Prog. Phys. **80**, 016503 (2017).
68. A. P. Alodjants and S. M. Arakelian, "Quantum chaos and its observation in coupled optical solitons," Zh. Eksp. i Teor. Fiz., 1995, **107**, 1792 (1995); transl. Sov. JETP, **80**, 995–1012 (1995).
69. S. Raghavan and G. P. Agrawal, "Switching and self-trapping dynamics of Bose-Einstein solitons," J. Mod. Opt. **47**, 1155–1169 (2000).
70. C. Sturm, D. Tanese, H.S. Nguyen, H. Flayac, E. Galopin, A. Lemaitre, I. Sagnes, D. Solnyshkov, A. Amo, G. Malpuech, J. Bloch, "All-optical phase modulation in a cavity-polariton Mach-Zehnder interferometer," Nature Comm. **5**, 3278 (2014).
71. C.W. Helstrom, *Quantum Detection and Estimation Theory, Mathematics in Science and Engineering,* (Academic, New York, 1976).
72. S. Haroche and J.-M. Raimond, *Exploring the Quantum,* (Oxford University, 2006).
73. C. C. Gerry, A. Benmoussa, and R. A. Campos, "Parity measurements, Heisenberg-limited phase estimation, and beyond," J. Mod. Opt. **54**, 2177 (2007).
74. L. Cohen, D. Istrati, L. Dovrat, and H. S. Eisenberg, "Super-resolved phase measurements at the shot noise limit by parity measurement," Optics Express **22**, 11945–11953 (2014).
75. T. Byrnes, Kai Wen, and Y. Yamamoto, "Macroscopic quantum computation using Bose-Einstein condensates," Phys. Rev. A **85**, 040306(R) (2012).
76. Ch. Weiss, S.L. Cornish, and S. A. Gardiner, "Superballistic center-of-mass motion in one-dimensional attractive Bose gases:Decoherence-induced Gaussian random walks in velocity space," Phys. Rev. A **93**, 013605 (2016).
77. Y. Sun, P. Wen, Y. Yoon, G. Liu, M. Steger, L. N. Pfeiffer, K. West, D. W. Snoke, and K. A. Nelson, "Bose-Einstein Condensation of Long-Lifetime Polaritons in Thermal Equilibrium," Phys. Rev. Lett. **118**, 016602 (2017).